

Sub-Eddington accreting supermassive primordial black holes explain Little Red Dots

Hai-Long Huang ^{1,2*}, Jun-Qian Jiang ^{2†}, Jibin He^{3‡}, Yu-Tong Wang^{1,2§} Yun-Song Piao^{1,2,4,5¶}

¹*School of Fundamental Physics and Mathematical Sciences, Hangzhou Institute for Advanced Study, UCAS, Hangzhou 310024, China*

²*School of Physical Sciences, University of Chinese Academy of Sciences, Beijing 100049, China*

³*Department of Physics and Chongqing Key Laboratory for Strongly Coupled Physics, Chongqing University, Chongqing 401331, P. R. China*

⁴*International Center for Theoretical Physics Asia-Pacific, Beijing/Hangzhou, China*

⁵*Institute of Theoretical Physics, Chinese Academy of Sciences, P.O. Box 2735, Beijing 100190, China*

Accepted XXX. Received YYY; in original form ZZZ

ABSTRACT

The James Webb Space Telescope (JWST) has uncovered an abundant population of compact, extremely red, and X-ray weak objects at $z \gtrsim 4$, known as “Little Red Dots” (LRDs). These objects exhibit spectral energy distributions that resemble both active galactic nuclei (AGN) and stellar population templates. However, whether dominated by AGN activity or compact star formation, the high redshifts and masses/luminosities of LRDs, coupled with their significant abundance, present potential challenges to the standard Λ CDM model. In this work, we propose a novel cosmic interpretation of this anomaly, suggesting that these LRDs are likely massive galaxies seeded by supermassive primordial black holes (SMPBHs) that came into being in the very early universe. We analyze 434 known LRDs from the 0.54 deg² COSMOS-Web survey and test the hypothesis that they originated from SMPBHs assuming sub-Eddington accretion. According to our result, SMPBHs actually could lead to the existence of more LRDs, even at higher redshifts ($z > 8$).

Key words: Early universe — Galaxy formation — Supermassive black holes

1 INTRODUCTION

The James Webb Space Telescope (JWST) offers an unprecedented glimpse into the early universe, extending the boundaries of detectable supermassive black holes (SMBHs) and their host galaxies in both redshift and mass (Larson et al. 2023; Übler et al. 2023b; Goulding et al. 2023; Kokorev et al. 2023; Übler et al. 2023a; Maiolino et al. 2023a; Bogdán et al. 2024; Natarajan et al. 2024; Kovács et al. 2024). Notably, JWST has revealed a previously unknown population of dust-reddened galaxies at redshifts $z \gtrsim 4$, so-called “Little Red Dots” (LRDs) (Harikane et al. 2023; Kocevski et al. 2023; Maiolino et al. 2023b; Killi et al. 2023; Matthee et al. 2024; Gentile et al. 2024; Pacucci & Narayan 2024; Feeney et al. 2024; Ma et al. 2024), posing new challenges to our understanding of early galaxy formation and SMBH growth. They have very red near-infrared colors and are very compact, with a median effective radius of ~ 150 pc, while some are even smaller with < 35 pc (Baggen et al. 2023; Furtak et al. 2023b; Pacucci & Loeb 2020). Additionally, these sources are abundant compared to the previously known population of high- z active galactic nuclei (AGN). Their number density is $10^{-4} - 10^{-5} \text{Mpc}^{-3} \text{mag}^{-1}$ at $z \sim 5$, and is 10 – 100 times more numerous than the faint end of quasar luminosity function (Greene et al. 2024).

Their physical interpretations bifurcated into two paths. The con-

tinuum emission in LRDs could be either dominated by the direct thermal emission from the accretion disk of AGN (Labbe et al. 2023a; Matthee et al. 2023), or from a population of young stars associated with vigorous star formation (Labbé et al. 2023b; Akins et al. 2023; Williams et al. 2024; Pérez-González et al. 2024; Audric Guia et al. 2024). However, if LRDs are dominated by star formation, they would dominate the high-mass end of the stellar mass function, and have central stellar mass densities significantly greater than the maximum observed at lower redshift (Akins et al. 2024). And based on their compact sizes, most of them must approach or exceed the maximal stellar mass surface densities observed in the local universe. By contrast, if LRDs are AGN-dominated, the high SMBH masses imply that the black hole-to-stellar mass ratio of LRDs is much higher than that in the local universe (Ananna et al. 2024), and an overabundance of SMBHs, about two orders of magnitude larger than was expected from pre-JWST observations of the bolometric quasar luminosity function (Kokorev et al. 2024; Kocevski et al. 2024; Casey et al. 2024).

There is actually clear evidence for AGN in the LRDs due to ubiquitous broad lines, and also evidence for evolved stellar populations with clear Balmer breaks (Greene et al. 2024; Wang et al. 2024). Therefore, LRDs could be a heterogeneous galaxy population, in which both AGN and star formation contribute to their fluxes to different degrees. However, Durodola et al. (2024) found that, independent of the specific AGN fraction adopted, the LRDs’ black holes are significantly overmassive relative to their host galaxies compared to the local $M_{\text{BH}} - M_*$ relation. Moreover, the first spectroscopic follow-ups showed a significant presence of broad emission lines in

* E-mail: huanghailong18@mails.ucas.ac.cn

† E-mail: jiangjunqian21@mails.ucas.ac.cn, jiangjq2000@gmail.com

‡ E-mail: 20242701016@stu.cqu.edu.cn

§ E-mails: wangyutong@ucas.ac.cn

¶ E-mail: yspiao@ucas.ac.cn

their spectra, suggesting the existence of AGN in their cores with a high M_{BH}/M_* ratio (Kocevski et al. 2023; Furtak et al. 2023a; Greene et al. 2024).

The existence of such overmassive black holes in the high-redshift Universe seems to provide the strongest evidence yet of heavy black hole seeding occurring during the cosmic dark ages. However, we propose that these SMBHs could have come into being in the very early universe as supermassive primordial black holes (SMPBHs). Recently, the cosmological implications of PBHs (Carr & Hawking 1974; Zel'dovich & Novikov 1967; Hawking 1971) have been intensively studied, see reviews by e.g. Carr et al. (2016); García-Bellido (2017); Sasaki et al. (2018); Carr & Kühnel (2020); Carr et al. (2021); Green & Kavanagh (2021); Carr & Kühnel (2021); Escrivà et al. (2022); Pi (2024); Domènech & Sasaki (2024). It is important to note that the required abundance of SMPBHs to explain the energy density of SMBHs can be compatible with current observations, see Figure 1 (see also Appendix A). These SMPBHs may originate from the direct collapse of large-amplitude non-Gaussian primordial perturbations after horizon entry (Byrnes et al. 2024; Nakama et al. 2018; Ünal et al. 2021; Gow et al. 2023; Hooper et al. 2024), or through other non-primordial-perturbation-like mechanisms e.g. Huang et al. (2023); Huang & Piao (2024). They can assemble galaxies through the seed effect¹ without requiring significant growth themselves.

The rest of this paper is structured as follows. In Section 2, we describe the COSMOS-Web survey and our data selection. In Section 3, we provide a comprehensive overview of the SMPBH model and present a detailed description of the data analysis methodology employed in this study. Lastly, we summarise our conclusions and offer a discussion of the implications in Section 4. Throughout this paper the values of cosmological parameters are set in light of the Planck results (Planck Collaboration et al. 2020).

2 DATA

We use a sample of $434 \lesssim z \lesssim 8$ LRDs selected from the 0.54 deg² COSMOS-Web JWST survey, as reported in Akins et al. (2024). COSMOS-Web is a major JWST Cycle 1 program that images a contiguous 0.54 deg² area using NIRCcam and a 0.19 deg² area with MIRI (Casey et al. 2023) within the COSMOS field (Scoville et al. 2007). For further details, refer to the original Ref. (Akins et al. 2024). The large sample size, which nearly doubles the number of LRDs reported in Kokorev et al. (2024); Kocevski et al. (2024), and the extensive on-sky area help minimize the impact of cosmic variance. This allows us to investigate whether SMPBHs could theoretically serve as seeds for galaxies with overmassive central black holes.

We present the properties of the partial COSMOS-Web LRDs in Table 1. These properties were derived based on two extreme scenarios: QSO models and galaxy models, where the LRD population is primarily composed of dust-reddened AGN or compact/dusty starbursts. In these models, it is assumed that the continuum emission in LRDs is dominated by flux from the accretion disk of AGN or from a population of young stars, respectively. Ideally, we would fit each object with a composite spectral energy distribution (SED) model that decomposes both components, as done in Durodola et al. (2024). However, as noted in Akins et al. (2024), the limited available

¹ The seed effect relates to the gravitational influence of individual black holes, while the Poisson effect accounts for the collective \sqrt{N} fluctuations in the number of black holes. See e.g. Hoyle & Narlikar (1966); Meszaros (1975); Carr & Silk (1983); Carr & Rees (1984); Carr & Silk (2018); Huang et al. (2024a); Dayal (2024) for more detail.

ID	QSO models			galaxy models	
	z_{qso}	$\log L_{\text{bol}}$ [erg s ⁻¹]	$\log M_{\text{BH}}$ [M_{\odot}]	z_{gal}	$\log M_*$ [M_{\odot}]
1491	6.2 ^{+1.2} _{-0.5}	46.2 ^{+0.4} _{-0.3}	10.1 ^{+0.4} _{-0.3}	6.1 ^{+1.2} _{-0.7}	10.7 ^{+0.3} _{-0.3}
3962	7.3 ^{+1.9} _{-1.8}	46.2 ^{+0.3} _{-0.4}	10.1 ^{+0.3} _{-0.4}	7.0 ^{+2.1} _{-2.3}	10.4 ^{+0.3} _{-0.2}
4056	6.0 ^{+1.0} _{-0.5}	45.8 ^{+0.2} _{-0.2}	9.7 ^{+0.2} _{-0.2}	6.2 ^{+2.2} _{-0.7}	9.4 ^{+0.3} _{-0.1}
8203	8.3 ^{+0.4} _{-0.4}	46.2 ^{+0.2} _{-0.3}	10.1 ^{+0.2} _{-0.3}	5.3 ^{+0.2} _{-0.2}	8.7 ^{+0.1} _{-0.1}
9430	7.3 ^{+1.0} _{-1.2}	45.9 ^{+0.3} _{-0.3}	9.8 ^{+0.3} _{-0.3}	7.8 ^{+0.6} _{-0.6}	9.8 ^{+0.2} _{-0.3}
9680	7.5 ^{+0.7} _{-1.4}	46.3 ^{+0.3} _{-0.3}	10.2 ^{+0.3} _{-0.3}	5.8 ^{+1.6} _{-0.4}	9.3 ^{+0.2} _{-0.2}
10023	6.0 ^{+1.0} _{-0.4}	45.3 ^{+0.2} _{-0.2}	9.2 ^{+0.2} _{-0.2}	6.0 ^{+2.3} _{-0.6}	8.9 ^{+0.2} _{-0.2}
10511	5.9 ^{+0.4} _{-0.3}	45.6 ^{+0.1} _{-0.1}	9.5 ^{+0.1} _{-0.1}	5.5 ^{+0.6} _{-0.3}	8.9 ^{+0.2} _{-0.1}
11737	7.8 ^{+1.5} _{-1.8}	46.5 ^{+0.5} _{-0.4}	10.4 ^{+0.5} _{-0.4}	7.5 ^{+1.7} _{-2.3}	10.7 ^{+0.7} _{-0.4}
13618	6.0 ^{+0.6} _{-0.5}	45.4 ^{+0.2} _{-0.2}	9.3 ^{+0.2} _{-0.2}	6.2 ^{+2.1} _{-0.8}	9.1 ^{+0.5} _{-0.3}
14599	5.9 ^{+0.4} _{-0.4}	45.5 ^{+0.2} _{-0.2}	9.4 ^{+0.2} _{-0.2}	5.6 ^{+2.1} _{-0.4}	8.9 ^{+0.3} _{-0.2}
15495	8.1 ^{+0.5} _{-0.7}	45.9 ^{+0.2} _{-0.2}	9.8 ^{+0.2} _{-0.2}	5.5 ^{+0.5} _{-0.3}	9.1 ^{+0.2} _{-0.1}
15654	5.7 ^{+0.4} _{-0.3}	46.2 ^{+0.2} _{-0.2}	10.0 ^{+0.2} _{-0.2}	5.6 ^{+0.6} _{-0.3}	9.8 ^{+0.2} _{-0.2}
15961	6.2 ^{+0.9} _{-0.5}	46.3 ^{+0.4} _{-0.3}	10.1 ^{+0.4} _{-0.3}	6.4 ^{+1.2} _{-0.6}	10.9 ^{+0.2} _{-0.4}
16108	6.0 ^{+1.3} _{-1.4}	45.8 ^{+0.2} _{-0.2}	9.7 ^{+0.2} _{-0.2}	5.6 ^{+0.5} _{-0.2}	9.2 ^{+0.2} _{-0.2}
16692	6.6 ^{+2.0} _{-1.3}	45.5 ^{+0.4} _{-0.4}	9.4 ^{+0.4} _{-0.4}	6.5 ^{+2.1} _{-1.5}	9.7 ^{+0.5} _{-0.4}
17632	7.7 ^{+1.1} _{-1.5}	46.0 ^{+0.4} _{-0.4}	9.9 ^{+0.4} _{-0.4}	6.9 ^{+1.8} _{-0.7}	10.3 ^{+0.6} _{-0.5}
18065	5.9 ^{+1.9} _{-0.5}	45.8 ^{+0.3} _{-0.4}	9.7 ^{+0.3} _{-0.4}	5.2 ^{+1.9} _{-0.7}	10.0 ^{+0.4} _{-0.4}
19068	6.5 ^{+2.1} _{-1.4}	45.2 ^{+0.3} _{-0.4}	9.1 ^{+0.3} _{-0.4}	6.7 ^{+2.0} _{-1.6}	9.4 ^{+0.4} _{-0.3}
26156	7.3 ^{+1.8} _{-1.5}	46.0 ^{+0.6} _{-0.5}	9.9 ^{+0.6} _{-0.5}	7.0 ^{+1.9} _{-1.8}	10.3 ^{+0.7} _{-0.5}
27062	6.1 ^{+1.8} _{-0.9}	45.3 ^{+0.4} _{-0.4}	9.2 ^{+0.4} _{-0.4}	5.7 ^{+2.2} _{-1.1}	9.4 ^{+0.5} _{-0.4}
27100	6.9 ^{+1.7} _{-1.2}	45.8 ^{+0.4} _{-0.4}	9.7 ^{+0.4} _{-0.4}	6.7 ^{+1.7} _{-1.6}	10.2 ^{+0.6} _{-0.5}
29753	6.0 ^{+1.6} _{-0.6}	45.6 ^{+0.2} _{-0.3}	9.5 ^{+0.2} _{-0.3}	6.8 ^{+1.5} _{-1.3}	9.6 ^{+0.3} _{-0.3}
36933	6.4 ^{+1.6} _{-0.9}	45.3 ^{+0.3} _{-0.3}	9.2 ^{+0.3} _{-0.3}	7.2 ^{+1.3} _{-1.5}	9.3 ^{+0.2} _{-0.3}
37490	6.5 ^{+1.8} _{-1.2}	45.6 ^{+0.3} _{-0.3}	9.4 ^{+0.3} _{-0.3}	6.4 ^{+1.9} _{-1.4}	9.5 ^{+0.3} _{-0.3}
39192	6.7 ^{+2.0} _{-1.1}	45.7 ^{+0.4} _{-0.4}	9.5 ^{+0.4} _{-0.4}	6.4 ^{+2.0} _{-1.5}	9.9 ^{+0.6} _{-0.4}
42832	7.6 ^{+1.7} _{-1.5}	46.0 ^{+0.5} _{-0.4}	9.9 ^{+0.5} _{-0.4}	7.9 ^{+1.4} _{-1.0}	10.4 ^{+1.0} _{-0.6}
42963	8.1 ^{+1.3} _{-1.9}	46.1 ^{+0.6} _{-0.5}	10.0 ^{+0.6} _{-0.5}	8.1 ^{+1.7} _{-2.3}	10.5 ^{+0.9} _{-0.6}
44171	7.2 ^{+2.0} _{-1.6}	45.9 ^{+0.4} _{-0.4}	9.8 ^{+0.4} _{-0.4}	6.9 ^{+1.9} _{-2.0}	10.1 ^{+0.4} _{-0.3}
46758	5.7 ^{+0.2} _{-0.2}	46.3 ^{+0.1} _{-0.1}	10.2 ^{+0.1} _{-0.1}	5.2 ^{+0.2} _{-0.2}	9.6 ^{+0.1} _{-0.1}
47467	5.4 ^{+0.3} _{-0.2}	46.2 ^{+0.2} _{-0.2}	10.1 ^{+0.2} _{-0.2}	5.4 ^{+0.4} _{-0.3}	9.9 ^{+0.2} _{-0.2}
47745	5.9 ^{+0.5} _{-0.4}	45.5 ^{+0.2} _{-0.2}	9.4 ^{+0.2} _{-0.2}	5.8 ^{+0.5} _{-0.5}	9.1 ^{+0.4} _{-0.3}
48256	6.3 ^{+1.8} _{-0.4}	46.3 ^{+0.1} _{-0.2}	10.2 ^{+0.1} _{-0.2}	5.7 ^{+0.7} _{-0.4}	9.6 ^{+0.2} _{-0.2}

Table 1. List of derived physical properties for the partial COSMOS-Web LRDs reported in Akins et al. (2024) (visit https://github.com/hollisakins/akins24_cw for the complete dataset, and we plot it in the $M_{\text{BH}} - M_*$ plane in Figure 2). Columns are as follows: (1) UNCOVER ID; (2) Redshift of the LRDs derived from QSO models; (3) Bolometric luminosity from QSO models; (4) SMBH mass inferred from the bolometric luminosity, assuming sub-Eddington accretion with $f_{\text{Edd}} = 0.01$; (5) Redshift of the LRDs based on galaxy models; (6) Stellar mass based on galaxy models.

information makes such an analysis prone to overfitting. Therefore, we use the results from the two models to estimate the corresponding SMBH mass and stellar mass, respectively.

The SMBH mass listed in Table 1 is inferred from the bolometric luminosity assuming sub-Eddington accretion. Specifically, we set the normalized accretion rate (Trakhtenbrot et al. 2011) as follows:

$$f_{\text{Edd}} \equiv \frac{L_{\text{bol}}}{L_{\text{Edd}}} = 0.01, \quad (1)$$

where the Eddington luminosity is defined by (Eddington 1926)

$$L_{\text{Edd}} = \frac{4\pi GMm_p c}{\sigma_T} \approx 1.3 \times 10^{38} \left(\frac{M}{M_{\odot}} \right) \text{ erg s}^{-1}, \quad (2)$$

where m_p is the proton mass, c is the speed of light and σ_T is the Thomson scattering cross-section. However, recent observations of high-redshift AGN suggest that many may be dormant, exhibiting sub-Eddington accretion rates (Jeon et al. 2023). For instance, Juodžbalis et al. (2024) report a SMBH with a mass of approximately $4 \times 10^8 M_{\odot}$, accreting at a rate of only 0.02 times the Eddington limit

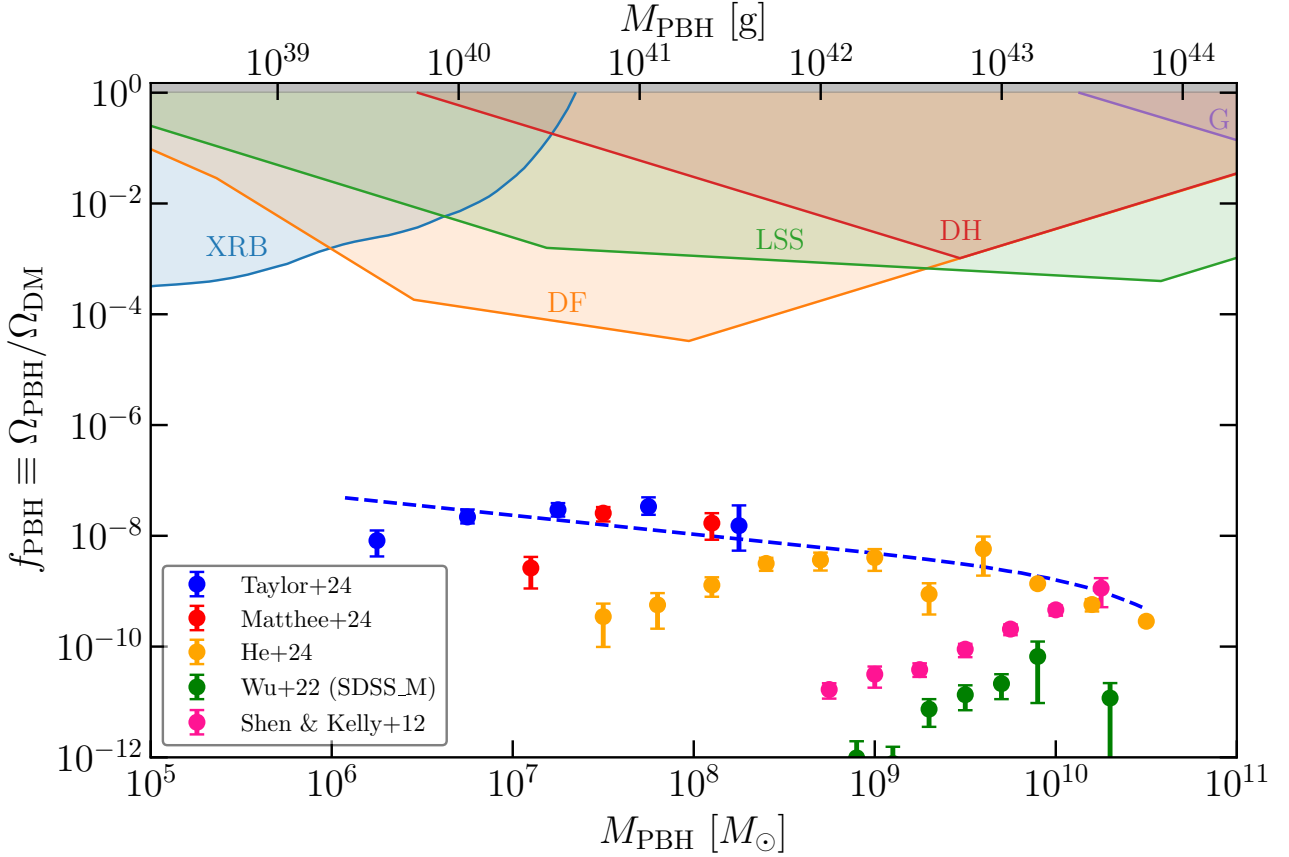


Figure 1. Comparison between the derived SMBH mass function and constraints on the fraction of SMPBHs in DM. The observational constraints are from heating of stars in the Galactic disk (DH), infalling of halo objects due to dynamical friction (DF), tidal disruption of galaxies (G), accretion limits come from X-ray binaries (XRB), and large-scale structure constraints (LSS) (Carr et al. 2021). Green points show the SMBH mass function at $z \sim 6$ from (Wu et al. 2022), and pink points show the SMBH mass function from (Shen & Kelly 2012), both derived from SDSS data. Yellow points show the SMBH mass function at $3.5 < z < 4.25$ derived from ground-based SDSS+HSC data in (He et al. 2024). Red points show the SMBH mass function derived from NIRCcam WFSS data in (Matthee et al. 2024). Blue points show the SMBH mass function at $3.5 < z < 6.0$ derived from data from the CEERS and RUBIES surveys (including LRDs) in (Taylor et al. 2024). Dashed blue curve shows a Schechter fit to the data in (Taylor et al. 2024) from $6.5 < \log M_{\text{BH}} < 8.5$ and the data in (He et al. 2024) at $\log M_{\text{BH}} > 8.5$.

(i.e. $f_{\text{Edd}} = 0.02$) at $z = 6.68$. Other relevant recent studies include e.g. Wu (2024); Weibel et al. (2024); Carnall et al. (2024); Siegel et al. (2024); Ni et al. (2024). In this context, the mass of a SMBH at a given bolometric luminosity is estimated to be greater, resulting in a larger black hole-to-stellar mass ratio. This is illustrated in Figure 2.

3 METHODS

3.1 The SMPBH model

The seeding of early galaxies by SMPBHs was investigated by Huang et al. (2024b). The method is outlined as follows.

After formed in the radiation-dominated era, the SMPBHs with mass M_i can bind to a dark matter (DM) halo in the subsequent matter-dominated era, with a mass given by (Carr & Silk 2018)

$$M_h = \frac{1 + z_{\text{eq}}}{1 + z} M_i \quad (3)$$

at redshift z . Its pregalactic growth is considered negligible (Huang et al. 2024a). The binding mass is derived from the fact that PBH fluctuations grow as $(1 + z)^{-1}$ during the matter-dominated era, but

this growth breaks down in the non-linear regime for $z < z_{\text{cut}}$. Then the mass growth rate of DM halos after z_{cut} with the mass of $M_h(z_{\text{cut}}) = (1 + z_{\text{eq}})/(1 + z_{\text{cut}}) M_i$ is characterized with an analytical function of the form (Fakhouri et al. 2010; Inayoshi et al. 2022)

$$\dot{M}_h \simeq 46.1 M_{\odot} \text{ yr}^{-1} \left(\frac{M_h}{10^{12} M_{\odot}} \right)^{1.1} (1 + 1.11z) \sqrt{\Omega_m (1 + z)^3 + \Omega_{\Lambda}}. \quad (4)$$

Its analytical solutions can be found in Appendix B. If we allow star formation to take place at z_{cut} , we have

$$M_* = \begin{cases} 0 & \text{if } z > z_{\text{cut}}, \\ \epsilon_* f_b M_h & \text{otherwise,} \end{cases} \quad (5)$$

where $f_b = \Omega_b/\Omega_m$ is the cosmic average fraction of baryons in matter and ϵ_* is the star formation efficiency that is assumed to be constant here.

On the other hand, the time evolution of the SMBH mass at $z < z_{\text{cut}}$

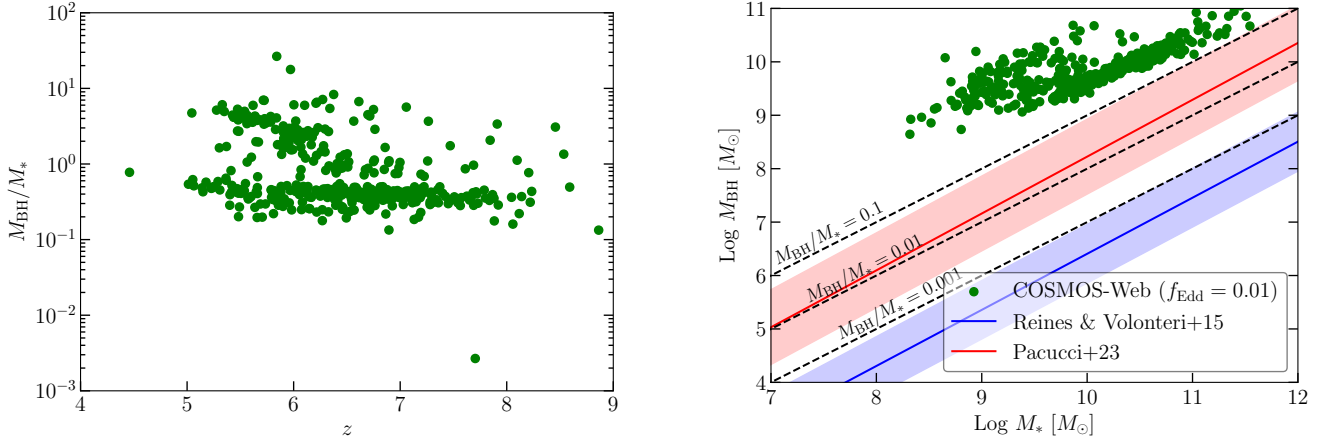


Figure 2. *Left panel:* Distribution of the LRDs’ black hole-to-star mass ratios at various redshifts assuming sub-Eddington accretion with $f_{\text{Edd}} = 0.01$. *Right panel:* The relationship between the SMBH masses and the stellar masses of LRDs (green points). The red line represents the high redshift $M_{\text{BH}} - M_*$ scaling relation with its intrinsic scatter (Pacucci et al. 2023), and the blue line represents the local scaling relation from (Reines & Volonteri 2015). Determining the location of these high- z systems in the $M_{\text{BH}} - M_*$ plane crucially depends on how the contributions from the stellar and the AGN components of the SEDs are evaluated.

can be expressed as

$$M_{\text{BH}}(t) = M_{\text{cut}} \exp \left[\frac{4\pi G m_p f_{\text{Edd}}}{c \sigma_T} \frac{1 - \epsilon}{\epsilon} (t - t_{\text{cut}}) \right]. \quad (6)$$

Here, $M_{\text{cut}} = M(z_{\text{cut}}) \simeq M_i$ is the SMPBH mass at z_{cut} and ϵ is the radiative efficiency. The cosmic time t and redshift z are related by

$$t(z) = \int_z^\infty \frac{dz'}{H(z')(1+z')}, \quad (7)$$

where $H(z)$ is the Hubble parameter. Here, we consider the sub-Eddington accretion with $f_{\text{Edd}} \ll 1$, and thus have $M_{\text{BH}}(z) = M_{\text{cut}} = M_i$ approximately. Therefore, in the SMPBH model with negligible accretion, the stellar mass $M_*(z)$ of a galaxy seeded by an SMPBH can be straightforwardly obtained using Equation 5. As an example, we plot the contour of the ratio of the SMBH mass to the stellar mass at $z = 5$ in the parameter space ($z_{\text{cut}}, \epsilon_*$) in the case of $M_i = M_{\text{BH}} = 10^9 M_\odot$ and $10^{11} M_\odot$ respectively in Figure 3.

3.2 Analysis of the BH mass-stellar mass relation

The hierarchical Bayesian analysis that allows us to go beyond individual events in order to study population properties (the $M_{\text{BH}} - M_*$ relation) is utilized in the analysis of LRDs.

In our model, the star formation efficiency, ϵ_* , is regarded as a redshift-independent constant. However, in reality, one should consider the impact of black hole accretion, as well as feedback from both black holes and TypeII Supernova (Dayal 2024). Therefore, ϵ_* should be understood as the redshift-averaged star formation efficiency. As mentioned, the stellar mass $M_*(z)$ of a galaxy seeded by an SMPBH can be straightforwardly obtained using Equation 5, we denote it as $F(z, M_{\text{BH}}; z_{\text{cut}}, \epsilon_*)$, however, due to various potential uncertainties in the model, we assume that the probability distribution of the stellar mass M_* at redshift z for a given SMBH mass M_{BH} follows a log-normal distribution parametrized by the mean $F(z, M_{\text{BH}}; z_{\text{cut}}, \epsilon_*)$ and the width σ :

$$\frac{dP(M_*|z, M_{\text{BH}}, \Lambda)}{d \log M_*} = \mathcal{N}(\log M_* | F(z, M_{\text{BH}}; z_{\text{cut}}, \epsilon_*), \sigma), \quad (8)$$

where the set of hyper-parameters $\Lambda = (\sigma, z_{\text{cut}}, \epsilon_*)$ describes the galaxy population seeded by SMPBHs and $\mathcal{N}(x|\bar{x}, \sigma)$ denotes the probability density of a Gaussian distribution with mean \bar{x} and variance σ^2 .

In our Markov chain Monte Carlo analysis, $\theta \equiv \{z, M_{\text{BH}}, M_*\}$ constitutes the parameters that define the individual LRD event. We fit the parameters σ, z_{cut} and ϵ_* to the measured data. The likelihood function is

$$\begin{aligned} \mathcal{L}(\mathbf{d}|\Lambda) \propto & \prod_j \int d \log M_* dz d \log M_{\text{BH}} \frac{dP(M_*|z, M_{\text{BH}}, \Lambda)}{d \log M_*} \\ & \times \mathcal{N}(\log M_* | \log M_{*,j}, \sigma_{*,j}) \mathcal{N}(z|z_j, \sigma_{z,j}) \\ & \times \mathcal{N}(\log M_{\text{BH}} | \log M_{\text{BH},j}, \sigma_{\text{BH},j}), \end{aligned} \quad (9)$$

where the product is over the data points, $M_{*,j}, z_j$ and $M_{\text{BH},j}$ denote the mean measured stellar masses, redshifts and SMBH masses, and we assume that the posteriors of the stellar mass, redshift and SMBH mass measurements are log-normal and uncorrelated.

4 RESULTS AND DISCUSSION

In our analysis, we employ uniform priors for each parameter: σ in the range $[0, 4]$, z_{cut} in the range $[4, 20]$, and $\log \epsilon_*$ in the range $[-10, 0]$. We report the Bayesian posterior distribution of parameters in Figure 4. The median value of the parameters together with their 90% equal-tailed credible intervals are $\sigma = 0.53^{+0.04}_{-0.03}$, $z_{\text{cut}} = 8.91^{+0.09}_{-0.03}$ and $\log \epsilon_* = -2.73^{+0.05}_{-0.06}$. It is noted that the cut-off redshift z_{cut} is constrained to be $z_{\text{cut}} > 8.87$. This is because star formation is assumed to occur only at $z < z_{\text{cut}}$, and the maximum redshift of the LRDs in our analysis is approximately ~ 8.86 (see the left panel of Figure 2). And the required star formation efficiency is fully compatible with the results estimated in Stefanon et al. (2021).

In this work, we present a novel explanation for the anomalies associated with LRDs by invoking SMPBHs. Unlike conventional astrophysical seed mechanisms, which often require sustained (super-)Eddington accretion, SMPBHs that came into being during the radiation-dominated era offer a more natural and efficient pathway to

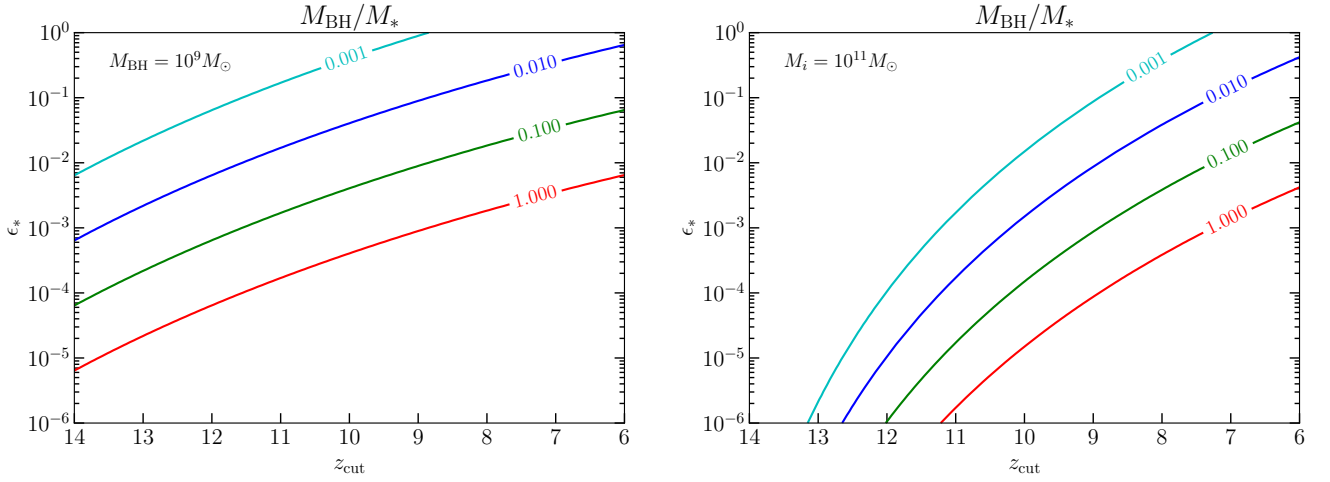


Figure 3. Left panel: Contour of the ratio of the SMBH mass to the stellar mass $z = 5$ in the parameter space ($z_{\text{cut}}, \epsilon_*$) in the case of $M_i = M_{\text{BH}} = 10^9 M_\odot$. Right panel: Same as the left panel with the different parameters $M_{\text{BH}} = 10^{11} M_\odot$.

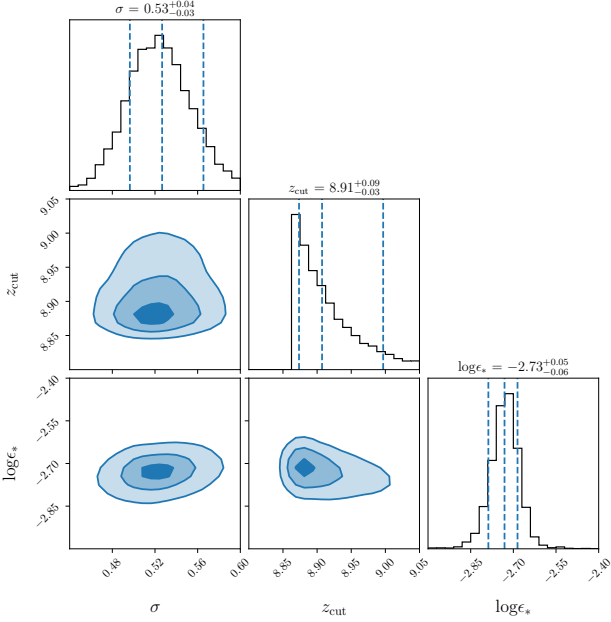


Figure 4. The posterior distribution of the Bayesian parameter estimation. The contours in the 2D distribution represent 1σ , 2σ and 3σ regions respectively.

the origin of the massive SMBHs observed in high-redshift galaxies. Additionally, SMPBHs can act as catalysts for early structure formation through the seed effect, providing a straightforward explanation for the unexpectedly high number density of LRDs without the need for intricate astrophysical processes. Based on a simple model, we demonstrate that galaxies seeded by SMPBHs can readily attain the elevated black hole-to-stellar mass ratios recently revealed in the COSMOS-Web survey (Akins et al. 2024). We further show that the extreme masses of these SMPBH-seeded galaxies imply that only a low star formation efficiency ($\log \epsilon_* \sim -2.73$) is required to account for their stellar mass.

A larger sample of red and compact objects at high redshift, coupled with improved understanding of the uncertainties in their black

hole and stellar mass measurements, is crucial for confirming the existence of this extraordinary population of overmassive black holes and their broader cosmological implications. We have shown that the hypothesis that these high-redshift massive galaxies are seeded by SMPBHs is supported by several considerations. However, our analysis focuses solely on the SMPBH scenario and it is important to explore a quantitative comparison with intermediate-mass PBH models (e.g. Dayal 2024) and astrophysical models (e.g. Prole et al. 2024). The deeper observations across X-ray, mid/far-IR, and radio wavelengths will be essential to accurately depict the intrinsic properties of LRDs (Akins et al. 2024), which helps us to distinguish the origin of SMBHs. The relevant issues will be left for the future to investigate

A refined SMPBH model that incorporates numerical simulations (e.g. Zhang et al. 2024b; Jeon et al. 2024; Zhang et al. 2024a) and accounts for more realistic astrophysical environments will also be important for advancing our understanding. Such studies could offer critical insights into the role of PBHs in early structure formation and help clarify the mechanisms responsible for producing these SMBHs in the high-redshift ($z \gtrsim 4$) universe.

DATA AVAILABILITY

The data underlying this article will be shared upon request to the corresponding author(s).

SOFTWARE

This research made use of `numpy` (Harris et al. 2020, <https://numpy.org>), `matplotlib` (Hunter 2007, <https://matplotlib.org/>) and `emcee` (Foreman-Mackey et al. 2013, <https://github.com/dfm/emcee/>).

ACKNOWLEDGEMENTS

We would like to thank Dashuang Ye for useful discussions. We are also thankful for the observations made with the NASA/ESA/CSA

James Webb Space Telescope and the public data available in https://github.com/hollisakins/akins24_cw. This work is supported by National Key Research and Development Program of China (Grant No. 2021YFC2203004), NSFC (Grant No.12075246), and the Fundamental Research Funds for the Central Universities.

REFERENCES

- Akins H. B., et al., 2023, *ApJ*, **956**, 61
- Akins H. B., et al., 2024, *arXiv e-prints*, p. [arXiv:2406.10341](https://arxiv.org/abs/2406.10341)
- Ananna T. T., Bogdán Á., Kovács O. E., Natarajan P., Hickox R. C., 2024, *ApJ*, **969**, L18
- Audric Guia C., Pacucci F., Kocevski D. D., 2024, *arXiv e-prints*, p. [arXiv:2408.11890](https://arxiv.org/abs/2408.11890)
- Baggen J. F. W., et al., 2023, *ApJ*, **955**, L12
- Bogdán Á., et al., 2024, *Nature Astronomy*, **8**, 126
- Byrnes C. T., Lesgourgues J., Sharma D., 2024, *J. Cosmology Astropart. Phys.*, **2024**, 012
- Carnall A. C., et al., 2024, *arXiv e-prints*, p. [arXiv:2405.02242](https://arxiv.org/abs/2405.02242)
- Carr B. J., Hawking S. W., 1974, *MNRAS*, **168**, 399
- Carr B., Kühnel F., 2020, *Annual Review of Nuclear and Particle Science*, **70**, 355
- Carr B., Kühnel F., 2021, *arXiv e-prints*, p. [arXiv:2110.02821](https://arxiv.org/abs/2110.02821)
- Carr B. J., Rees M. J., 1984, *MNRAS*, **206**, 801
- Carr B. J., Silk J., 1983, *ApJ*, **268**, 1
- Carr B., Silk J., 2018, *MNRAS*, **478**, 3756
- Carr B., Kühnel F., Sandstad M., 2016, *Phys. Rev. D*, **94**, 083504
- Carr B., Kohri K., Sendouda Y., Yokoyama J., 2021, *Reports on Progress in Physics*, **84**, 116902
- Casey C. M., et al., 2023, *ApJ*, **954**, 31
- Casey C. M., Akins H. B., Kokorev V., McKinney J., Cooper O. R., Long A. S., Franco M., Manning S. M., 2024, *arXiv e-prints*, p. [arXiv:2407.05094](https://arxiv.org/abs/2407.05094)
- Dayal P., 2024, *arXiv e-prints*, p. [arXiv:2407.07162](https://arxiv.org/abs/2407.07162)
- Domènech G., Sasaki M., 2024, *Classical and Quantum Gravity*, **41**, 143001
- Durodola E., Pacucci F., Hickox R. C., 2024, *arXiv e-prints*, p. [arXiv:2406.10329](https://arxiv.org/abs/2406.10329)
- Eddington A. S., 1926, *The Internal Constitution of the Stars*
- Escrivà A., Kühnel F., Tada Y., 2022, *arXiv e-prints*, p. [arXiv:2211.05767](https://arxiv.org/abs/2211.05767)
- Fakhouri O., Ma C.-P., Boylan-Kolchin M., 2010, *MNRAS*, **406**, 2267
- Feeney J., Kavanagh P., Regan J. A., 2024, *arXiv e-prints*, p. [arXiv:2409.13441](https://arxiv.org/abs/2409.13441)
- Foreman-Mackey D., Hogg D. W., Lang D., Goodman J., 2013, *PASP*, **125**, 306
- Furtak L. J., et al., 2023a, *arXiv e-prints*, p. [arXiv:2308.05735](https://arxiv.org/abs/2308.05735)
- Furtak L. J., et al., 2023b, *ApJ*, **952**, 142
- García-Bellido J., 2017, in *Journal of Physics Conference Series*. IOP, p. 012032 ([arXiv: 1702.08275](https://arxiv.org/abs/1702.08275)), doi:10.1088/1742-6596/840/1/012032
- Gentile F., et al., 2024, *arXiv e-prints*, p. [arXiv:2408.10305](https://arxiv.org/abs/2408.10305)
- Goulding A. D., et al., 2023, *ApJ*, **955**, L24
- Gow A. D., Assadullahi H., Jackson J. H. P., Koyama K., Vennin V., Wands D., 2023, *EPL (Europhysics Letters)*, **142**, 49001
- Green A. M., Kavanagh B. J., 2021, *Journal of Physics G Nuclear Physics*, **48**, 043001
- Greene J. E., et al., 2024, *ApJ*, **964**, 39
- Harikane Y., et al., 2023, *ApJ*, **959**, 39
- Harris C. R., et al., 2020, *Nature*, **585**, 357
- Hawking S., 1971, *MNRAS*, **152**, 75
- He W., et al., 2024, *ApJ*, **962**, 152
- Hooper D., Ireland A., Krnjaic G., Stebbins A., 2024, *J. Cosmology Astropart. Phys.*, **2024**, 021
- Hoyle F., Narlikar J. V., 1966, *Proceedings of the Royal Society of London Series A*, **290**, 177
- Huang H.-L., Piao Y.-S., 2024, *Phys. Rev. D*, **110**, 023501
- Huang H.-L., Cai Y., Jiang J.-Q., Zhang J., Piao Y.-S., 2023, *arXiv e-prints*, p. [arXiv:2306.17577](https://arxiv.org/abs/2306.17577)
- Huang H.-L., Jiang J.-Q., Piao Y.-S., 2024a, *arXiv e-prints*, p. [arXiv:2407.15781](https://arxiv.org/abs/2407.15781)
- Huang H.-L., Wang Y.-T., Piao Y.-S., 2024b, *arXiv e-prints*, p. [arXiv:2410.05891](https://arxiv.org/abs/2410.05891)
- Hunter J. D., 2007, *Computing in Science & Engineering*, **9**, 90
- Inayoshi K., Harikane Y., Inoue A. K., Li W., Ho L. C., 2022, *ApJ*, **938**, L10
- Jeon J., Liu B., Bromm V., Finkelstein S. L., 2023, *MNRAS*, **524**, 176
- Jeon J., Bromm V., Liu B., Finkelstein S. L., 2024, *arXiv e-prints*, p. [arXiv:2402.18773](https://arxiv.org/abs/2402.18773)
- Juodžbalis I., et al., 2024, *arXiv e-prints*, p. [arXiv:2403.03872](https://arxiv.org/abs/2403.03872)
- Killi M., et al., 2023, *arXiv e-prints*, p. [arXiv:2312.03065](https://arxiv.org/abs/2312.03065)
- Kocevski D. D., et al., 2023, *ApJ*, **954**, L4
- Kocevski D. D., et al., 2024, *arXiv e-prints*, p. [arXiv:2404.03576](https://arxiv.org/abs/2404.03576)
- Kokorev V., et al., 2023, *ApJ*, **957**, L7
- Kokorev V., et al., 2024, *ApJ*, **968**, 38
- Kovács O. E., et al., 2024, *ApJ*, **965**, L21
- Labbe I., et al., 2023a, *arXiv e-prints*, p. [arXiv:2306.07320](https://arxiv.org/abs/2306.07320)
- Labbe I., et al., 2023b, *Nature*, **616**, 266
- Larson R. L., et al., 2023, *ApJ*, **953**, L29
- Ma Y., et al., 2024, *arXiv e-prints*, p. [arXiv:2410.06257](https://arxiv.org/abs/2410.06257)
- Maiolino R., et al., 2023a, *arXiv e-prints*, p. [arXiv:2305.12492](https://arxiv.org/abs/2305.12492)
- Maiolino R., et al., 2023b, *arXiv e-prints*, p. [arXiv:2308.01230](https://arxiv.org/abs/2308.01230)
- Matthee J., et al., 2023, *arXiv e-prints*, p. [arXiv:2306.05448](https://arxiv.org/abs/2306.05448)
- Matthee J., et al., 2024, *ApJ*, **963**, 129
- Meszáros P., 1975, *A&A*, **38**, 5
- Nakama T., Carr B., Silk J., 2018, *Phys. Rev. D*, **97**, 043525
- Natarajan P., Pacucci F., Ricarte A., Bogdán Á., Goulding A. D., Cappelluti N., 2024, *ApJ*, **960**, L1
- Ni Y., Chen N., Zhou Y., Park M., Yang Y., DiMatteo T., Bird S., Croft R., 2024, *arXiv e-prints*, p. [arXiv:2409.10666](https://arxiv.org/abs/2409.10666)
- Pacucci F., Loeb A., 2020, *ApJ*, **895**, 95
- Pacucci F., Narayan R., 2024, *arXiv e-prints*, p. [arXiv:2407.15915](https://arxiv.org/abs/2407.15915)
- Pacucci F., Nguyen B., Carniani S., Maiolino R., Fan X., 2023, *ApJ*, **957**, L3
- Pérez-González P. G., et al., 2024, *ApJ*, **968**, 4
- Pi S., 2024, *arXiv e-prints*, p. [arXiv:2404.06151](https://arxiv.org/abs/2404.06151)
- Planck Collaboration et al., 2020, *A&A*, **641**, A6
- Prole L. R., Regan J. A., Whalen D. J., Glover S. C. O., Klessen R. S., 2024, *arXiv e-prints*, p. [arXiv:2410.06141](https://arxiv.org/abs/2410.06141)
- Reines A. E., Volonteri M., 2015, *ApJ*, **813**, 82
- Sasaki M., Suyama T., Tanaka T., Yokoyama S., 2018, *Classical and Quantum Gravity*, **35**, 063001
- Scoville N., et al., 2007, *ApJS*, **172**, 1
- Shen Y., Kelly B. C., 2012, *ApJ*, **746**, 169
- Siegel J., et al., 2024, *arXiv e-prints*, p. [arXiv:2409.11457](https://arxiv.org/abs/2409.11457)
- Stefanon M., Bouwens R. J., Labbé I., Illingworth G. D., Gonzalez V., Oesch P. A., 2021, *ApJ*, **922**, 29
- Taylor A. J., et al., 2024, *arXiv e-prints*, p. [arXiv:2409.06772](https://arxiv.org/abs/2409.06772)
- Trakhtenbrot B., Netzer H., Lira P., Shemmer O., 2011, *ApJ*, **730**, 7
- Übler H., et al., 2023a, *arXiv e-prints*, p. [arXiv:2312.03589](https://arxiv.org/abs/2312.03589)
- Übler H., et al., 2023b, *A&A*, **677**, A145
- Ünal C., Kovetz E. D., Patil S. P., 2021, *Phys. Rev. D*, **103**, 063519
- Wang H., Piao Y.-S., 2024, *arXiv e-prints*, p. [arXiv:2404.18579](https://arxiv.org/abs/2404.18579)
- Wang B., et al., 2024, *ApJ*, **969**, L13
- Weibel A., et al., 2024, *arXiv e-prints*, p. [arXiv:2409.03829](https://arxiv.org/abs/2409.03829)
- Williams C. C., et al., 2024, *ApJ*, **968**, 34
- Wu P.-F., 2024, *arXiv e-prints*, p. [arXiv:2409.00471](https://arxiv.org/abs/2409.00471)
- Wu J., et al., 2022, *MNRAS*, **517**, 2659
- Ye G., Piao Y.-S., 2020, *Phys. Rev. D*, **101**, 083507
- Zel'dovich Y. B., Novikov I. D., 1967, *Soviet Astron. AJ (Engl. Transl.)*, **10**, 602
- Zhang S., Bromm V., Liu B., 2024a, *arXiv e-prints*, p. [arXiv:2405.11381](https://arxiv.org/abs/2405.11381)
- Zhang S., Liu B., Bromm V., 2024b, *MNRAS*, **528**, 180

A COMPATIBILITY OF THE SMPBH ABUNDANCE WITH CURRENT OBSERVATIONS

It is well-known that the abundance of SMPBHs is strictly limited by cosmological and astrophysical observations. In this Appendix, we will check whether the required abundance of SMPBHs to explain the energy density of SMBHs is compatible with current observations.

Recently, many collaborations have constructed the SMBH mass function, $\Phi(M_{\text{BH}})$, using different sample (e.g. Taylor et al. 2024; Matthee et al. 2024; He et al. 2024; Wu et al. 2022; Shen & Kelly 2012). To achieve this, they divide the SMBH mass range into several bins with widths denoted as $\Delta \log \left(\frac{M_{\text{BH}}}{M_{\odot}} \right)$ (Here for convenience we will refer to it as $\Delta \log M_{\text{BH}}$ and this convention has been used throughout the text). Then each SMBH is fractionally assigned to these mass bins according to its posterior distribution. The mass function is constructed by dividing the weighted object count in each bin by the bin width and the comoving volume. An example of the result can be seen in the Figure 12 of Taylor et al. (2024).

Assuming that all the SMBHs are of primordial origin, we can convert their mass function into the fraction of DM,

$$f_{\text{PBH}}(M_{\text{PBH}}) \equiv \frac{\Omega_{\text{PBH}}(M_{\text{PBH}})}{\Omega_{\text{DM}}} = \Delta \log M_{\text{BH}} \times \frac{\Phi(M_{\text{BH}})M_{\text{BH}}}{\rho_{\text{DM}}}. \quad (10)$$

We compare the results with current observational constraints on f_{PBH} in Figure 1. It is obvious that the required abundance of SMPBHs to explain the energy density of SMBHs is consistent with existing upper limits.

B ANALYTICAL SOLUTION FOR HALO MASS GROWTH

The solution of the ordinary differential equation

$$\frac{dy(x)}{dx} = [y(x)]^{\nu} f(x) \quad (11)$$

is given by

$$y(x) = \left\{ [y(x_0)]^{1-\nu} - (-1+\nu) \int_{x_0}^x f(x') dx' \right\}^{\frac{1}{1-\nu}}. \quad (12)$$

According to Equation 4, the mass growth rate of DM halos after z_{cut} is given by

$$\frac{d}{dz} \left(\frac{M_h}{M_{\odot}} \right) \simeq \left(\frac{M_h}{M_{\odot}} \right)^{1.1} f(z), \quad (13)$$

where

$$f(z) = -0.042 \times \frac{1 + 1.11z}{1 + z}. \quad (14)$$

We use the fact that

$$\frac{dt}{dz} = -\frac{1}{H_0 \sqrt{\Omega_m (1+z)^3 + \Omega_{\Lambda}}} \frac{1}{1+z}, \quad (15)$$

where H_0 is the Hubble constant. Throughout this paper our cosmological parameters are set in the corresponding Planck values (Planck Collaboration et al. 2020), and we do not consider the effect of the Hubble tension on H_0 and relevant results (e.g. Ye & Piao 2020; Wang & Piao 2024), which may be actually negligible. Therefore, the analytical solutions of Equation 4 is

$$\frac{M_h(z)}{M_{\odot}} = \left\{ \left[\frac{M_h(z_{\text{cut}})}{M_{\odot}} \right]^{-0.1} - 0.004662(z_{\text{cut}} - z) + 0.000462 \ln \left(\frac{1 + z_{\text{cut}}}{1 + z} \right) \right\}^{-10}. \quad (16)$$

This paper has been typeset from a \LaTeX file prepared by the author.